Nakajima et al. Progress in Earth and Planetary Science (2017) 4:2
DOI 10.1186/s40645-017-0117-x

Progress in Earth and Planetary Science

RESEARCH ARTICLE Open Access

Model depiction of the atmospheric flows of radioactive cesium emitted from the Fukushima Daiichi Nuclear Power Station accident

Teruyuki Nakajima[1,2*], Shota Misawa[1], Yu Morino[3], Haruo Tsuruta[1,4], Daisuke Goto[3], Junya Uchida[1], Toshihiko Takemura[5], Toshimasa Ohara[3], Yasuji Oura[6], Mitsuru Ebihara[6] and Masaki Satoh[1]

Abstract

In this study, a new method is proposed for the depiction of the atmospheric transportation of the ^{137}Cs emitted from the Fukushima Daiichi Nuclear Power Station accident. This method employs a combination of the results of two aerosol model ensembles and the hourly observed atmospheric ^{137}Cs concentration at surface level during 14–23 March 2011 at 90 sites in the suspended particulate matter monitoring network. The new method elucidates accurate transport routes and the distribution of the surface-level atmospheric ^{137}Cs relevant to eight plume events that were previously identified. The model ensemble simulates the main features of the observed distribution of surface-level atmospheric ^{137}Cs. However, significant differences were found in some cases, and this suggests the need to improve the modeling of the emission scenario, plume height, wet deposition process, and plume propagation in the Abukuma Mountain region. The contributions of these error sources differ in the early and dissipating phases of each event, depending on the meteorological conditions.

Keywords: Fukushima Nuclear Power Station accident, Aerosols, Radioactive materials, ^{137}Cs, Chemical transport modeling, Ensemble models

Introduction

A wide area of northeastern Japan, the Tohoku and Kantou regions, was contaminated by the radioactive material emitted from the accident at the Fukushima Daiichi Nuclear Power Station (FDNPS) of the Tokyo Electric Power Company (TEPCO), as manifested by various environmental investigations (Nakajima et al. 2014). The accident was caused by the Great East Japan Earthquake, which struck at 14:46 Japan Standard Time (JST; Coordinated Universal Time, UTC+ 9 h) on 11 March 2011.

Takemura et al. (2011) show that the negative anomaly of a 500-hPa height over the Okhotsk Sea area along 145° E made the westerly jet stronger than the climatological mean during mid-March; consequently, 70 to 80% of the radioactive material from the FDNPS was driven to the Pacific Ocean and the rest of the globe (Takemura et al. 2011; Stohl et al. 2012; Mészáros et al. 2016). The remaining material spread over and deposited onto the land area of Japan, producing characteristic hot spot patterns (Yasunari et al. 2011; JAEA 2012; SCJ 2014). The total emission of ^{137}Cs into the atmosphere until the end of April was estimated to be 14.6 ± 3.5 PBq (SCJ 2014). The ratio of the total deposition over the Japanese land area to the total atmospheric emission was estimated as 20 ± 6%, according to the airborne monitoring conducted by the Ministry of Education, Culture, Sports, Science, and Technology, Japan (MEXT 2011), whereas the ratio was calculated as 27 ± 10% based on the multi-model intercomparison by the Science Council of Japan (SCJ 2014). To date, this inconsistency has not been fully understood, owing to the lack of observation data, which is attributable to instrumental damage and electric outages

* Correspondence: terry-nkj@nifty.com
[1]Atmosphere and Ocean Research Institute (AORI), The University of Tokyo, 5-1-5 Kashiwanoha, Kashiwa, Chiba 277-8568, Japan
[2]Earth Observation Research Center (EORC), Japan Aerospace Exploration Agency (JAXA), 2-1-1 Sengen, Tsukuba, Ibaraki 305-8505, Japan
Full list of author information is available at the end of the article

as well as modeling uncertainties. In addition, there is still great uncertainty in the emission time series of the radioactive material, as shown in Fig. 1. Yumimoto et al. (2016) conducted an inverse analysis to optimally estimate the emission rate using the time series of the deposition map, but the result is very different from that of Katata et al. (2015).

Recently, Tsuruta et al. (2014) developed a method to directly measure the hourly time series of the atmospheric ^{137}Cs concentration at surface level, from the aerosol sampling tapes of the national suspended particulate matter (SPM) network. The SPM network monitors air pollution by employing beta-ray attenuation counters. Four laboratories, namely, those of Tokyo Metropolitan University, the Nuclear Professional School of the University of Tokyo, the Japan Atomic Energy Agency, and the Japan Chemical Analysis Center, retrieved the atmospheric loading from the hourly aerosol spots on the SPM tape. This method offers the potential for studying the atmospheric transport of ^{137}Cs, although the data is from surface level, during the entire post-accident period; the SPM dataset has high temporal and spatial sampling, with observations every hour at 90 out of 400 sites (Fig. 2). In Fig. 2, it can be seen that the Nakadori region is a channel basin area between the Ou and Abukuma mountains, while the Hamadori region is a coastal region to the east of the Abukuma mountains. The FDNPS is located in the northern part of the Hamadori region. In this report, we compare the ensemble results of two aerosol transport models with SPM data. An important purpose of the comparison is to investigate the validity of the combined use of SPM data and multi-model simulations to depict the transportation of atmospheric ^{137}Cs over the Japan land area. Once validated, further analysis can be performed on a larger volume of SPM data, such as the most recent data from 99 SPM sites, which has recently been made available to the public (Oura et al. 2015). In addition, the results could be a useful input for our second model intercomparison, which is intended as a follow-up to the first comparison, which was made by the SCJ (SCJ 2014), and this can contribute to future discussions of the use of models in emergency protocols.

Tsuruta et al. (2014) identified nine plumes, as listed in Fig. 3, that transported particulates to the land area of Japan and in which the maximum atmospheric ^{137}Cs concentration exceeded 10 Bq m^{-3}, based on a synoptic analysis using a time series of the SPM data and the wind vector field. For purposes of comparison, we selected plumes P2 to P9 in the period 14–24 March 2011. In this period, there were two migrations of low pressure systems over Japan; these occurred on 15 and 20 March, according to the weather maps shown in Fig. 4.

Methods/Experimental

Model simulation of the atmospheric ^{137}Cs concentration at surface level

In this study, two aerosol transport models were employed to simulate the atmospheric transportation of ^{137}Cs. The first model uses an online dynamic core of the nonhydrostatic icosahedron atmospheric model (NICAM; Tomita and Satoh 2004; Satoh et al. 2008) coupled with the spectral radiation-transport model for aerosol species (SPRINTARS; Takemura et al. 2000; Dai et al. 2014); we will refer to this as the N-model. The NICAM model is implemented with an air-mass flux-type dynamic scheme of high mass conservation, and it can cover a global-to-regional simulation with its three grid systems, which include a quasihomogeneous global grid, a stretched grid, and a diamond regional grid (Uchida et al. 2015). We adopted the diamond grid system for a regional simulation with the following settings: 10 s time step, 5-km grid resolution, and 40 layers, with the lowest layer being 20 m thick. The cloud microphysics scheme was the NICAM single-moment scheme with six water categories (NSW6), which is a simplified version of Lin's scheme (Lin et al. 1983). The turbulent diffusion calculation adopted a partial condensation scheme (Mellor and Yamada 1982) and an eddy diffusion scheme with a level 2.0 turbulent scale adjustment scheme (Nakanishi and Niino 2004). The numerical domain was a rhombus area, with apexes at 26.5° N, 144.4° E; 35.8° N, 132.0° E; 50.6° N, 133.4° E; and 39.9° N, 147.7° E; it covered the Tohoku region (the northeastern part of the Japanese islands, including the Fukushima and Miyagi prefectures, as shown in Fig. 2) and the Kantou Plain region (the area including the Tokyo, Saitama, Chiba, Kanagawa, and Ibaraki prefectures). After release from the FDNPS, the atmospheric ^{137}Cs was treated as a sulfate aerosol particle

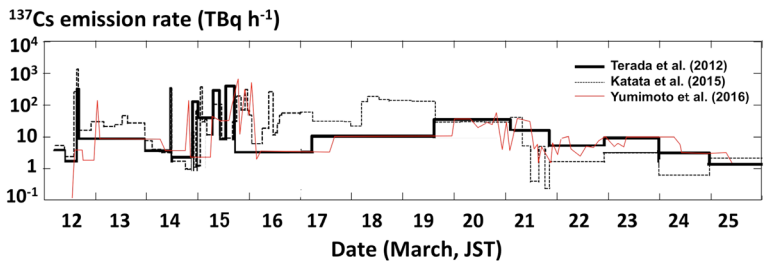

Fig. 1 Time series of the ^{137}Cs emission rate from the FDNPS, as estimated by Terada et al. (2012), Katata et al. (2015), and Yumimoto et al. (2016)

Fig. 2 Names of key regions and locations of SPM sites at the time of accident for the present study. The Tohoku region is the northeastern part of the Japanese islands and includes the Fukushima and Miyagi prefectures; the Kantou region is the area that includes the Tokyo, Saitama, Chiba, Kanagawa, and Ibaraki prefectures. The FDNPS is located in the northern part of the Hamadori region, a coastal area to the east of the Abukuma Mountains. The Nakadori region is a channel basin area between the Ou and the Abukuma mountains. *Open circles* are SPM monitoring sites managed and maintained by local governments in eastern Japan before the accident. The base map was modified by using the original map in Fig. 1 of Tsuruta et al. (2014)

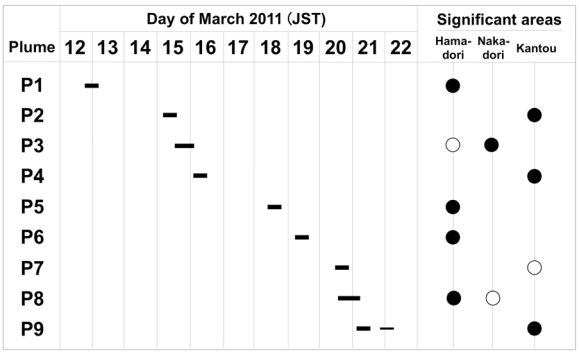

Fig. 3 Plumes identified by Tsuruta et al. (2014). *Horizontal bars* show the period with high ^{137}Cs concentrations (>10 Bq m^{-3}). *Closed and open circles* indicate areas in the Hamadori, Nakadori, and Kantou regions where the concentrations were larger or smaller, respectively, than 100 Bq m^{-2}

and assumed to undergo transportation, hygroscopic growth, dry and wet deposition, and gravitational settling, according to the scheme of Takemura et al. (2000). The present numerical experiment assumed a monodisperse sulfate-equivalent particle with a radius of 0.24 μm, taking into account the observed size distribution by Kaneyasu et al. (2012) and an in-cloud scavenging coefficient defined by Takemura et al. (2000) as 0.8 (Goto et al. 2015a).

The other model was a meteorological model, the weather research and forecast model (WRF) version 3.1 (Skamarock et al. 2008), coupled with a three-dimensional chemical transport model, the Models-3 Community Multiscale Air Quality (CMAQ) version 4.6 (Byun and Schere 2006); we will refer to this as the W-model. The CMAQ had been modified for radioactive material transport by the National Institute for Environmental Studies for a FDNPS simulation (Morino et al. 2011; SCJ 2014). We employed the WRF modules of scalar positive-definite advection, full diffusion, without the sixth-order horizontal-advection noise filter, and the planetary boundary parameterization of the Mellor-Yamada-Janjic scheme (Wang et al. 2012). In the present simulation, all the ^{137}Cs was assumed to be in particulate phase (Sportisse 2007), and the chemical and aerosol processes were not calculated because no detailed process has been well reported. The deposition schemes were those of Byun and Ching (1999) and Byun and Schere (2006). The mean particle radius was assumed to

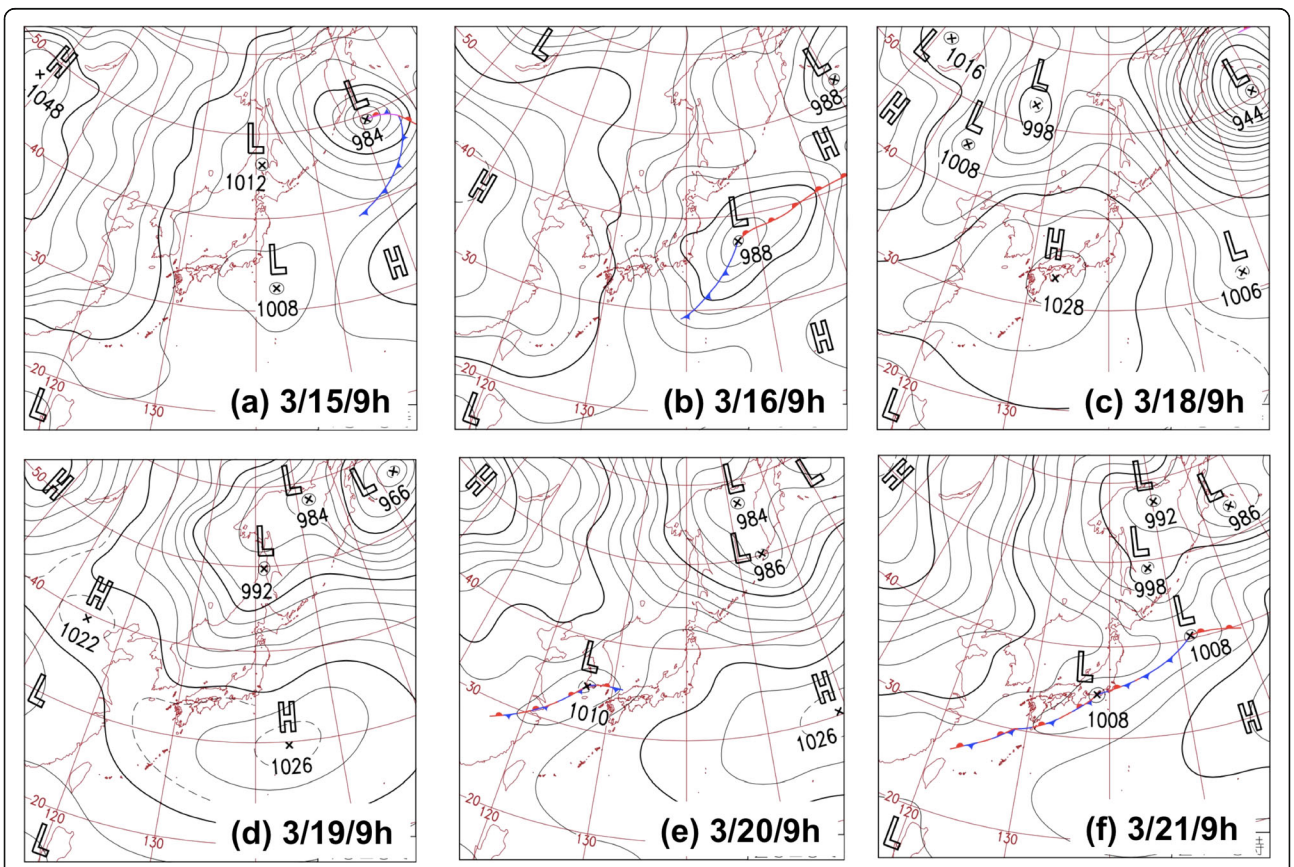

Fig. 4 a–f Weather maps based on JMA analysis at 9:00 JST in the analysis period

be 0.5 μm, and the geometrical dispersion σ_g was assumed to be 1.1 (Sparmacher et al. 1993; Sportisse 2007; Kaneyasu et al. 2012). The model domain was a 700×700 km^2 area, covering most of the Tohoku and Kantou regions, with a grid resolution of 3 km and 34 layers, with the lowest layer approximately 60 m thick. The simulation period was 14–24 March, and the analysis was performed by comparing the model ensemble results with the observed atmospheric ^{137}Cs concentration at surface level. The total deposition over Japanese land was simulated as 2.12 PBq by the N-model and 2.21 PBq by the W-model (Morino et al. 2013). These values belong to the small deposition group in the SCJ model comparison (SCJ 2014), which gave a mean value of total deposition of 2.92 PBq.

Both models were nudged with three-hourly 5×5 km mesoscale objective analysis data (MANAL) from the Japan Meteorological Agency (JMA). We selected the emission scenario of Terada et al. (2012), which has been used in many previous studies and is thus suitable for comparison with them. Figure 5 shows two examples of the simulated and observed atmospheric ^{137}Cs used to study the performance of both the N- and the W-model for specific cases, taken from the detailed time sequences as shown in Figs. 6 and 7 with precipitation maps of the JMA analysis and the N-model. These two examples were 15 March, 12:00 JST (3/15/12 h), and 21 March, 9:00 JST (3/21/9 h), when high-concentration plumes of more than 100 Bq m^{-3} were observed in the Kantou region. In Fig. 5, observed concentrations are indicated by color-coded circles, and the data below the detection limit of 0.1 Bq m^{-3} are indicated by triangles. On 15 March, a dry process governed the transportation, and there was no significant precipitation until late that evening, as indicated by the JMA analysis shown in Fig. 6. The distribution of the atmospheric ^{137}Cs was well simulated by the two models for a wide range of concentrations, from 0.1 to 100 Bq m^{-3}. It should be noted that the observed high-concentration area was confined to a narrow region, which was consistent with the simulated plume-wise distribution starting from the FDNPS for the Kantou region. The plumes simulated by the N-model were less diffused (narrower) than those simulated by the W-model. Judging by the correlation coefficients of the observed and simulated distributions, reality is assumed to fall between these two results; this is further discussed in the following paragraph.

For the March 21 event, the results of the N- and W-models differed significantly, as can be seen in Fig. 5c, d, respectively. Morning precipitation occurred in the Kantou region on 21 March, as will be shown in Fig. 7b. However, the simulated atmospheric concentration of ^{137}Cs was generally smaller than the observed values, suggesting that the simulated wet deposition was too strong for the W-model. Wet deposition during the total period over land in Japan was simulated as 1.68 and 2.12 PBq by the N- and W-model, respectively.

As indicated in Fig. 5, the accuracies of the simulated plume patterns of the two models differed from event to event. These differences were also reported by SCJ (2014). One way to reconcile the differences and construct statistically optimum distributions is to use a multi-model ensemble method to calculate the weighted mean concentration $\overline{C}_k$ for the kth grid point of the N-model at the jth time step, as given by

$$\overline{C}_{k,j} = \left(\frac{C_{\mathrm{N},k,j}}{\sigma_{\mathrm{N}}^2} + \frac{C_{\mathrm{W},k,j}}{\sigma_{\mathrm{W}}^2}\right) \Big/ \left(\frac{1}{\sigma_{\mathrm{N}}^2} + \frac{1}{\sigma_{\mathrm{W}}^2}\right), \quad (1)$$

where $C_{N,k,\mathrm{j}}$ and $C_{W,k,j}$ are the values of the N- and W-model, respectively. The grid values of the W-model are linearly interpolated onto the N-model grid. The quantities σ_{N} and σ_{W} are the daily root mean square deviations of the respective model values from the observed values. Figure 8 shows a comparison of the observed values with the values obtained by the N-model alone and with the two-model ensemble means constructed by the proposed method. The daily correlation coefficients for specific days (15, 20, and 21 March) are listed in Table 1. The correlation coefficients were calculated using the daily means of the observed and simulated values at the surface level, as linearly interpolated at the site locations. The ensemble method constructs an atmospheric ^{137}Cs distribution that had a correlation coefficient better than that of either model alone. However, 20 March was an exception; the correlation coefficient of the two-model ensemble method was not as good as that of the N-model, although it was superior to that of the W-model. The 3-day average of the correlation coefficients was improved to 0.51 by the two-model ensemble method, from 0.48 obtained with the N-model and 0.46 with the W-model.

Results and discussion

Structure of atmospheric ^{137}Cs plumes

In this section, we examine the plume formation and dissipation during each of three periods: 15–16 March, 18–19 March, and 20–21 March 2011.

15–16 March

Land plume events in the Kantou and Tohoku regions lasted from the morning of 15 March until noon of the next day. Time sequences of the ^{137}Cs concentration of the two models and the observations are shown in Fig. 6a, b, along with precipitation maps of the JMA analysis and those of the N-model. Two-model ensemble means and the wind vectors of the JMA analysis are shown in Fig. 9 for several characteristic times. During the morning of 15 March, a low-pressure system with a weak trough structure was located in the Pacific region off the Kantou region (Fig. 4a). A northeasterly wind